ADVANCED MATERIALS
www.advmat.de

Soft Multifunctional Composites and Emulsions with Liquid Metals

*Navid Kazem, Tess Hellebrekers, and Carmel Majidi**

Binary mixtures of liquid metal (LM) or low-melting-point alloy (LMPA) in an elastomeric or fluidic carrier medium can exhibit unique combinations of electrical, thermal, and mechanical properties. This emerging class of soft multifunctional composites have potential applications in wearable computing, bio-inspired robotics, and shape-programmable architectures. The dispersion phase can range from dilute droplets to connected networks that support electrical conductivity. In contrast to deterministically patterned LM microfluidics, LMPA- and LM-embedded elastomer (LMEE) composites are statistically homogenous and exhibit effective bulk properties. Eutectic Ga-In (EGaIn) and Ga-In-Sn (Galinstan) alloys are typically used due to their high conductivity, low viscosity, negligible nontoxicity, and ability to wet to nonmetallic materials. Because they are liquid-phase, these alloys can alter the electrical and thermal properties of the composite while preserving the mechanics of the surrounding medium. For composites with LMPA inclusions (e.g., Field's metal, Pb-based solder), mechanical rigidity can be actively tuned with external heating or electrical activation. This progress report, reviews recent experimental and theoretical studies of this emerging class of soft material architectures and identifies current technical challenges and opportunities for further advancement.

1. Introduction

Progress in emerging domains like wearable computing, soft robotics, and biohybrid engineering depends on new classes of soft multifunctional materials that match the mechanical properties of natural biological tissue. Efforts to combine thermal and electrical functionality with mechanical compliance and elasticity have largely focused on elastomer composites,[1,2] graft copolymers,[3] and a variety of deterministic architectures.[4,5] The latter includes soft microfluidic[6,7] and microsolidic[8] systems in which an elastomer is embedded with microchannels of a fluid or low-melting-point material.

In recent years, there have been attempts to merge these various approaches to create hybrid material architectures that exhibit novel combinations of mechanical, thermal, and electrical properties. Of particular interest has been the use of liquid metal (LM) and low-melting-point alloys (LMPAs). Referring to **Figure 1**, LM systems span a wide range of length scales and architectures: mm-scale channels embedded in elastomer[8,9] (Figure 1A,B), traces deposited on a substrate with a pressurized syringe[10] (Figure 1C), microscale traces printed with soft lithography[11] (Figure 1D), LM droplets[12,13] (Figure 1E,F), microscale droplets embedded in a polysiloxane[14] (Figure 1G), and LM nanospheres synthesized with ultrasonication (Figure 1H).[15] Composites composed of droplets suspended in a continuous elastic phase can be tailored to exhibit a unique and extraordinary combination of mechanical, electrical, and thermal properties. Although still in its nascent stages, these LMPA- and LM-embedded elastomer (LMEE) composites have the potential for transformative impact in application domains that require multifunctional materials that are soft and highly deformable.

Here we present an overview of recent studies on binary mixtures of an LM or LMPA dispersion phase in an elastomeric or fluidic carrier medium. This includes special focus on LMEEs and the interplay of composition, microstructure, deformation, and mesoscale material properties for this emerging materials class. Following a brief background (Section 1.1) and materials overview (Section 1.2), we report on progress in the following subdomains:

- **Ga-based LM dispersions**: mechanical, dielectric, and thermal properties (Section 2);
- **Connected LM networks**: electrical conductivity and electromechanical coupling (Section 3);
- **Connected LMPA networks**: rigidity tuning and shape changing (Section 4).

Such work relates to a rich body of research on the synthesis, characterization, and theory of statistically uniform dispersions in a continuous phase.[16–19] It also builds on efforts from the last decade to combine LM or LMPAs with soft microfluidics to create mechanically robust electronics[8,20] and elastomers capable of changing mechanical rigidity.[21] Whenever relevant, we will highlight the connection between recent advancements

N. Kazem, T. Hellebrekers, Prof. C. Majidi
Integrated Soft Materials Lab
Carnegie Mellon University Pittsburgh
Pittsburgh, PA 15213, USA
E-mail: cmajidi@andrew.cmu.edu

DOI: 10.1002/adma.201605985

in LM-based compositions and these more established domains.

1.1. Background

Since the early 2000s, there has been remarkable progress in new classes of soft and stretchable electronics that are mechanically robust and compatible with human tissue.[5] Many of these technologies incorporate metalized textiles,[22] conductive conjugated polymers,[23–29] and rubbery nanocomposites composed of a percolating network of metal nanoparticles or carbon allotropes embedded in an elastomer.[17,30] There has also been rapidly growing interest in the use of 1D and 2D nanomaterials for flexible and stretchable electronics.[31–35] This includes 3D aerogels with carbon nanotubes[36] and Ag nanowires[37] (**Figure 2**A) and related efforts to perform Brownian dynamic simulations on generalized "patchy rods" networks (Figure 2B).[38] Other approaches to stretchable functionality are based on patterning thin metal films into wavy or serpentine shapes that can stretch through elastic bending or torsion.[4] A key advantage of this approach is that it can be extended to thin semiconductor films for stretchable np junctions and logic arrays.[39] Using novel lithography techniques, such materials can be integrated with conventional microelectronics for creating fully functional circuits on a stretchable carrier medium.[40–49]

In the last decade, there has also been extraordinary progress in the emerging field of soft-matter electronics with Ga-based LM alloys such as eutectic gallium-indium (EGaIn, Figure 2C) and gallium-indium-tin (Galinstan).[54–65] These alloys form a surface oxide that enables droplet "moldability"[50] (Figure 2D), electrochemical manipulation,[12] elastomer wetting for fluidic injection[20,51] (Figure 2E), and the synthesis of nanoscale droplets (Figure 2F).[52] In addition to LM, soft-matter electronics have been successfully demonstrated using ionic microfluidics[66–70] and hydrogels.[71–73] More generally, soft-matter electronics represent the class of electronic materials and circuits that are composed entirely of soft condensed matter, i.e., materials that deform under light mechanical loading. These heterogeneous systems typically use soft elastomer[74] as the continuous phase and exhibit bulk mechanical properties similar to that of soft biological tissue.

There have been several review articles that extensively cover the emerging field of Ga-based LM microfluidic electronics. The focus of these articles range from circuit and sensing applications[58,75,76] to emerging fabrication methods based on lithographic, additive, subtractive, and injection-based techniques.[60,64,77] More recent developments in LM microfluidics have been directed towards 3D printing of microfluidic channels[78,79] and applications of LM in antennas and resonators,[59,62,65,80–88] electrodes[89–91] and metamaterials.[92–94] In addition, there has been an increased focus on exploring different phenomena like electro-chemistry,[12,62,95–110] wettability, and interfaces[111–114] of LMs. Recent developments in stretchable electronics with LM is the focus of a companion report[115] and will not be reviewed here. Instead, this report will highlight progress in the development of soft multifunctional compositions that contain a random dispersion of LM[14] (Figure 2G) or LMPA[53] (Figure 2H) droplets embedded in a continuous phase.

Navid Kazem received his B.S. degree in civil engineering from the Sharif University of Technology (Iran) in 2012. He got his M.S. degree in civil and environmental engineering from Carnegie Mellon University in 2013 and is currently a PhD student working with the Integrated Soft Materials Laboratory under the supervision of Professor Carmel Majidi. His research focus is on multifunctional soft materials with liquid metals embedded in elastomers, for applications in wearable computing, stretchable electronics, and biomedical devices.

Tess Hellebrekers received her B.S. degree in biomedical engineering from the University of Texas at Austin in 2016. She is currently a PhD student at Carnegie Mellon University working with the Integrated Soft Materials Laboratory under the supervision of Professor Carmel Majidi. Her research focus is on a broad range of soft sensing for integration with underwater robotics.

Carmel Majidi is an associate professor of mechanical engineering at Carnegie Mellon University. He leads the Integrated Soft Materials Laboratory, which develops novel materials architectures, theoretical models, and fabrication methods for soft multifunctional composites and microfluidics. Professor Majidi's researches contribute to the fields of soft bioinspired robotics, wearable computing, and mechanics of soft matter. Prior to joining Carnegie Mellon University, he had postdoctoral fellowships at Princeton and Harvard. He received his B.S. degree from Cornell University and M.S. and Ph.D. degrees from UC Berkeley.

1.2. Materials Overview

Ga-based LM alloys such as eutectic gallium–indium (EGaIn; 75% Ga and 25% In by weight) and gallium–indium–tin (Galinstan; 68% Ga, 22% In, and 10% Sn) are popular LMs for soft microfluidic electronics.[20,50] Both alloys have a volumetric

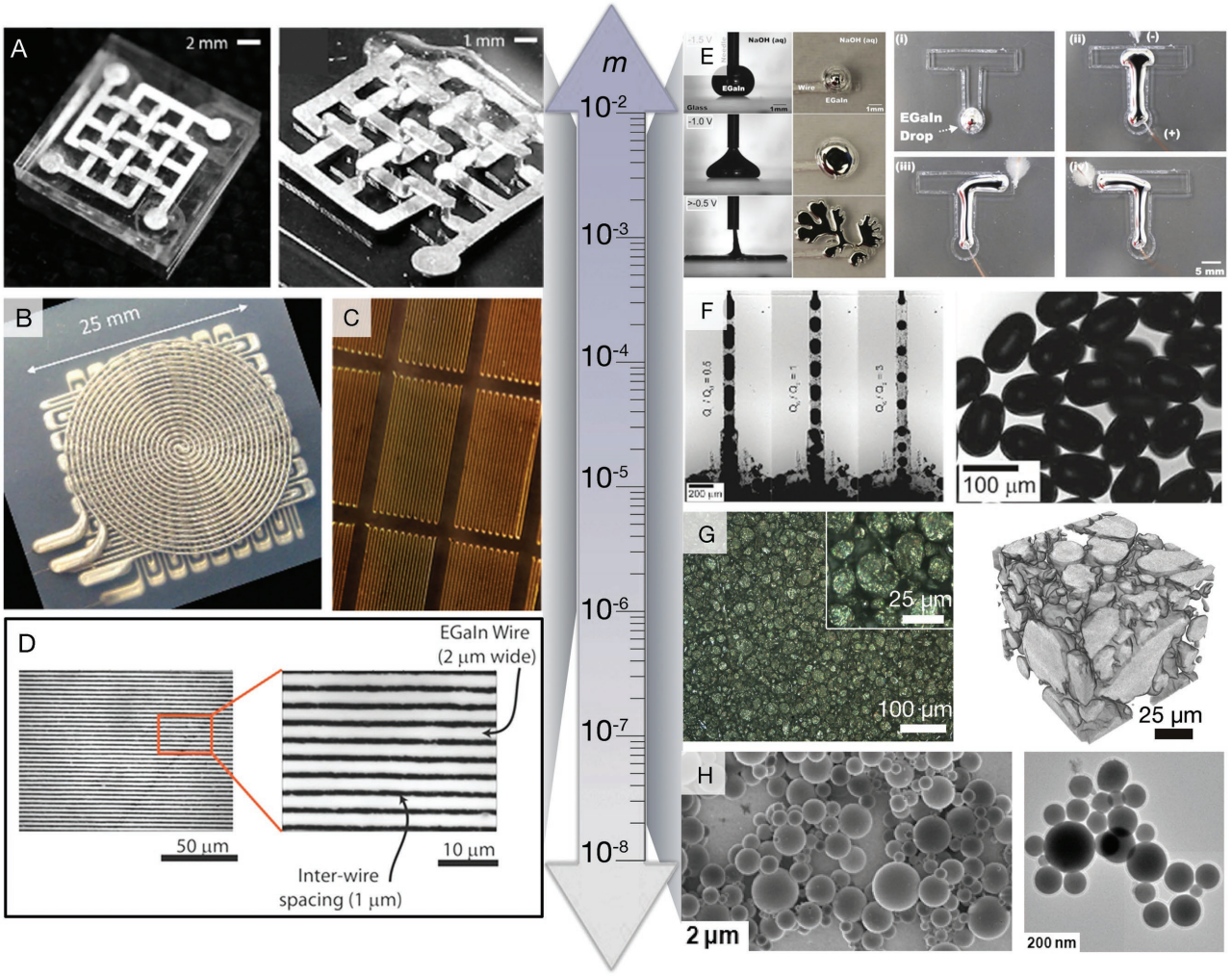

Figure 1. Applications of liquid metal alloy at different length scales. A) Microsolidics with LMPA embedded in polydimethylsiloxane (PDMS). Reproduced with permission,[8] Copyright 2007, Wiley-VCH. B) Strain and pressure sensing with microfluidic channels of LM in a soft elastomer. Reproduced with permission,[9] Copyright 2012, IEEE. C) EGaIn strain gauges produced by direct writing using a pressurized syringe. Reproduced with permission,[10] Copyright 2014, Wiley-VCH. D) Fabrication of microscale EGaIn traces with stamp lithography. Reproduced with permission,[11] Copyright 2014, Wiley-VCH. E) LM droplet manipulation with voltage-controlled wetting and electrochemistry. Reproduced with permission,[12] Copyright 2014, National Academy of Sciences. F) Synthesis of LM microdroplets with microfluidics. Reproduced with permission,[13] Copyright 2012, Wiley-VCH. G) Polydisperse EGaIn inclusions in a silicone elastomer. Reproduced with permission,[14] Copyright 2016, Wiley-VCH. H) Nanoscale LM droplets produced with ultrasonication. Reproduced with permission,[15] Copyright 2011, American Chemical Society.

electrical conductivity of 3.4×10^6 S m^{-1}[116] and thermal conductivity of 26.4 W m^{-1} K^{-1} at ≈30 °C.[117–119] Compared to Hg, Fr, Cs, and other metals that are liquid at (or near) room temperature, Ga-based alloys are especially attractive for their low viscosity (2 mPa s),[120] low toxicity,[121] and negligible vapor pressure. Moreover, in an oxygenated environment, they form a self-passivating Ga_2O_3 oxide skin that dramatically reduces its surface tension.[12,121,122] This oxide layer allows LM droplets to wet polymer surfaces and also has a role in suspension stabilization of an LM-liquid polymer emulsion. The Ga_2O_3 coating has a thickness of ≈0.5–3 nm[123,124] and behaves like an elastic membrane that can support a maximum surface stress of 0.5–0.6 N m^{-1}.[20,125] When broken, it reforms almost instantaneously – allowing the droplet to be structurally self-stabilizing and moldable.[50,126]

Pb-based LMPA has also been used as a conductive material for creating mechanically deformable electronics.[8,127] When heated, the molten solder is injected into a microfluidic channel embedded inside an elastomer and then allowed to solidify at room temperature. These so-called "microsolidic" devices are soft and flexible and represent an inexpensive method for rapid fabrication of flexible printed circuit boards. More recently, interest has extended to microsolidic material architectures that undergo substantial changes in mechanical rigidity.[21,53,128] This is accomplished by changing the phase of the embedded LMPA through internal Joule heating or the application of external heat. Instead of Pb-based solder, Field's metal is typically used due to its low melting point and negligible toxicity.

For applications of interest, LM alloys are typically embedded within an elastomer matrix. In general, elastomers can be

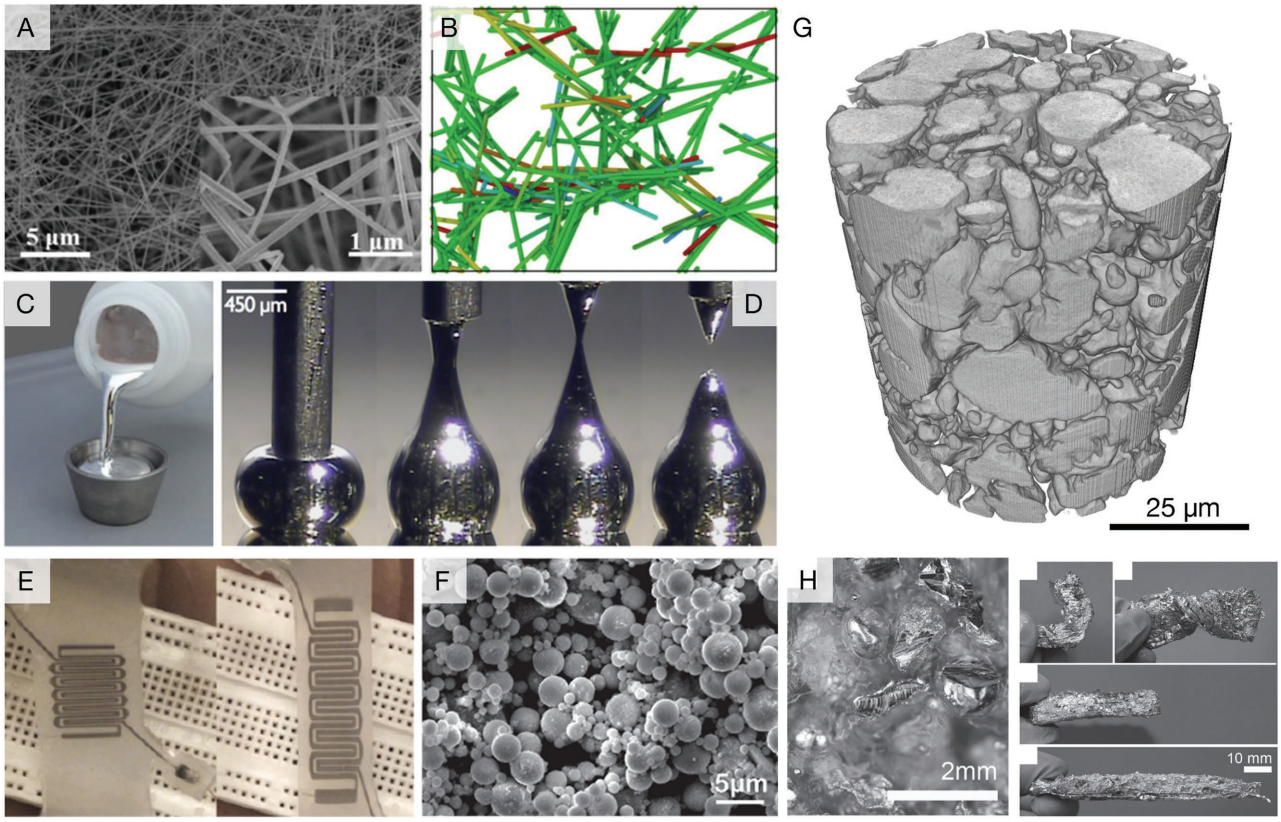

Figure 2. A) 3D network of silver nanowire. Reproduced with permission,[37] Copyright 2012, Nature Publishing Group. B) Brownian dynamic simulation of rigid patchy rods showing percolation path at 30% strain. Reproduced with permission,[38] Copyright 2015, Royal Society of Chemistry. C) Eutectic gallium-indium (EGaIn) alloy is liquid at room temperature (Indium Corp.). D) Deposition of EGaIn showing "moldability" through formation of Ga_2O_3 skin. Reproduced with permission,[50] Copyright 2008, Wiley-VCH. E) Stretching an interdigitated capacitor composed of an EGaIn channel embedded in soft silicone elastomer. Reproduced with permission,[51] Copyright 2013, Institute of Physics. F) SEM image of EGaIn nanoparticles produced with ultrasonication. Reproduced with permission,[52] Copyright 2014, Wiley-VCH. G) Nano-CT scan of polydisperse LM inclusions in elastomer. Adapted from Bartlett et al.[14] H) Rigidity-tuning foam composed of a connected LMPA network embedded in elastomer. Reproduced with permission,[53] Copyright 2016, Wiley-VCH.

selected for a range of rigidities – from that of soft fatty tissue[69,79] and skin[129] (elastic modulus ≈ 1–100 kPa) to ligaments and tendons[11,67,92] (>10 MPa; Shore Hardness >20 A). Polysiloxanes such as Pt-catalyzed poly(dimethylsiloxane) (PDMS) are often used as a carrier medium due to their low modulus (≈0.1–1 MPa) and high strain limit (>200%).[130] Popular commercial brands include Sylgard 184 (Dow Corning), Ecoflex 30 (Smooth-On), and Elastosil (Wacker). There has also been interest in soft polyurethanes,[14] polyacrylates (e.g., 3M VHB),[131] and block copolymer elastomers like styrene ethylene butylene styrene.[132]

2. LM Dispersions

A popular method to tailor the electrical, thermal, and mechanical properties of elastomers is to embed them with rigid particles that have the desired bulk properties.[17,133,134] This results in a particle-filled composite with mesoscale properties that typically exhibit some combination of the material properties of the dispersion phase and medium. In some cases, emergent properties are observed that are not exhibited by the constituent materials, particularly in relation to material anisotropies and strain-induced couplings. However, while promising for low-load or moderate-strain applications, introducing rigid filler in a soft matrix material will lead to a significant decrease in strain limit and an increase in rigidity and inelastic behavior.[135] A similar change in mechanical properties is also observed with co-polymers in which polymer groups with desired electrical or thermal properties are grafted to elastomeric macromolecules.[136] In general, such degradation can arise from the internal impedance mismatch between the constituents and becomes more pronounced with higher weight ratios of the dispersion phase.[137–139] Nonetheless, particle-filled elastomers and graft copolymers will continue to have a central role in soft-matter engineering and represent an exciting opportunity for advancing the field of stretchable electronics.

To preserve the mechanical properties of the elastomer matrix, EGaIn droplets are used in place of rigid filler particles.[14,140–142] Because the inclusions are liquid-phase, their presence does not significantly change the mechanical properties of the host elastomer. As a result, these LMEE composites can be engineered to have a unique combination of elastic, electrical, and thermal properties (**Figure 3**). More generally,

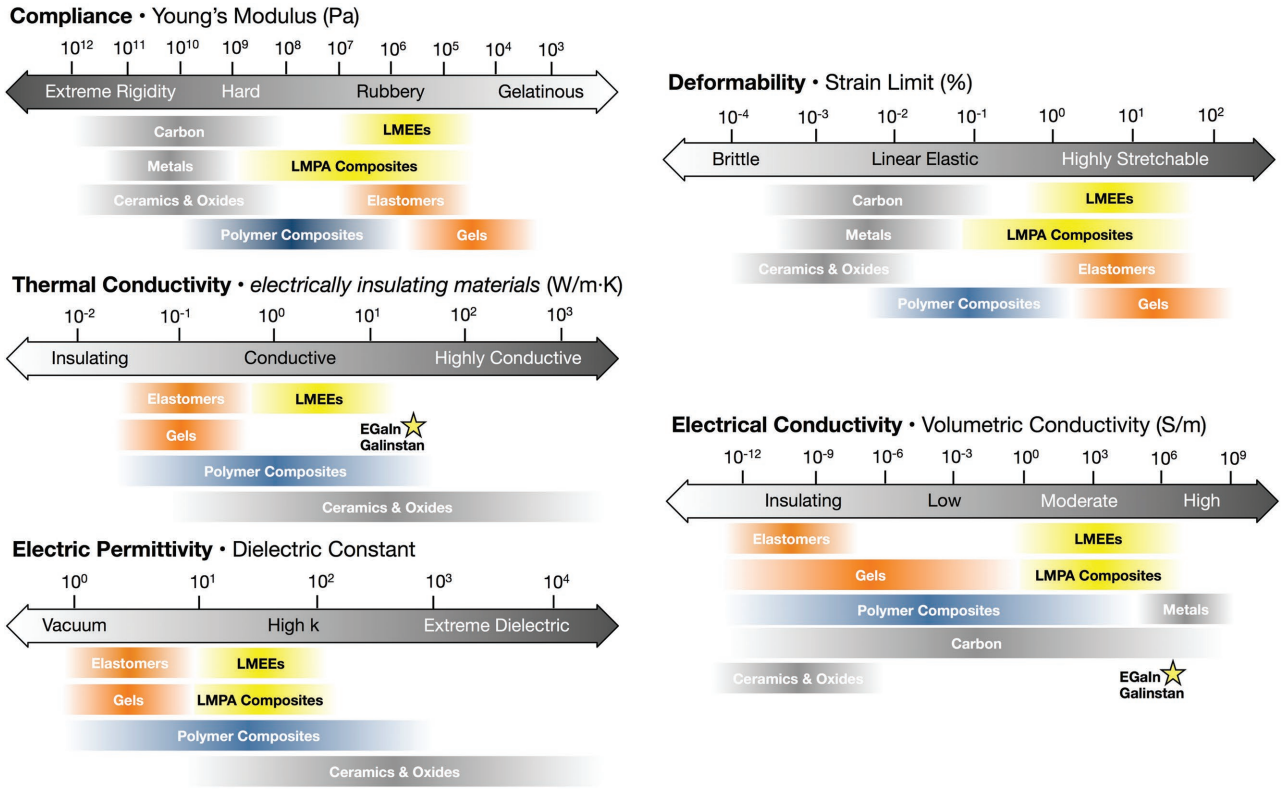

Figure 3. Comparison of LMPA and LMEE composites with other material properties (adapted from other sources[14,140,141]).

LM droplets can be created through a variety of techniques, including molding[143] (**Figure 4**A), use of acoustic waves[144] (Figure 4B), microfluidic flow-focusing[145,146] (Figure 4C), shear-mixing[14,147] (Figure 4D,E), and sonication[15,64,148,149] (Figure 4F,G). As shown in Figure 4, the LM particle size can range from mm scale (Figure 4A) to tens and hundreds of nm (Figure 4H). With sonication, the diameter of nanodroplets can be controlled by sonication time (Figure 4I), temperature (Figure 4J) and concentration of acid and surfactant (Figure 4K). For these droplets to be embedded in elastomer, more study will be required to examine the potential influence of the oxide skin and use of surfactant in preparing an emulsion with liquid polymer.

2.1. Mechanical Properties

In contrast to many other elastomer composites with dense particle dispersions, LMEEs can be soft and highly stretchable (**Figure 5**A). In the case of EGaIn droplets in silicone, it has been shown that the strain limit (ε_m) and elastic modulus (E) of the composite has only limited dependency on inclusion volume fraction (ϕ).[14] Referring to Figure 5B, composites with a polydisperse suspension of 1–10 µm diameter EGaIn droplets in soft polysiloxane (Ecoflex 00-30; Smooth-On) exhibit a strain limit $\varepsilon_m \approx 600\%$ for all values of ϕ. Moreover, E is observed to increase by a modest amount (from 75 to 90 kPa) as ϕ increases from 0 to 0.5. Interestingly, this relatively small increase in stiffness appears to contradict Eshelby's Theory of Inclusions, which suggests that a composite with liquid inclusions should have an effective modulus of $E_c = E/(1 + 5\phi/3)$.[153] Recently, Style et al. have reported an experimentally measured stiffening effects observed for elastomers embedded with a dilute dispersion of fluidic droplets with high surface tension.[154,155] In those studies, the elastic stiffening is explained with a modified Eshelby theory that takes surface tension (γ) of the liquid droplets into consideration

$$E_c = E\left\{\frac{1+\frac{5\gamma}{2ER}}{(1-\phi)\frac{5\gamma}{2ER}+\left(1+\frac{5\phi}{3}\right)}\right\} \quad (1)$$

where R is the droplet radius. In this modified Eshelby formulation, the stiffness of the composite is influenced by both the entropic response of the polymeric carrier medium and the change in free surface/interfacial energy of the fluidic dispersion phase. Such a correction has also been extended to model soft-matter multi-phase composites in the non-dilute limit using a mean-field Mori-Tanaka homogenization technique, also referred to as an equivalent inclusion-average stress (EIAS) method.[156,157] While the surface tension of Ga-based LM is high, the formation of the Ga_2O_3 skin can cause the effective surface tension to be quite low.[12,122] Nonetheless, elongation of LM droplets will require the creation of new surfaces and this can influence mechanical stiffness, at least in the first loading cycle. For subsequent loading, the skin may crumple and behave like a wrinkled thin-walled shell. To examine this

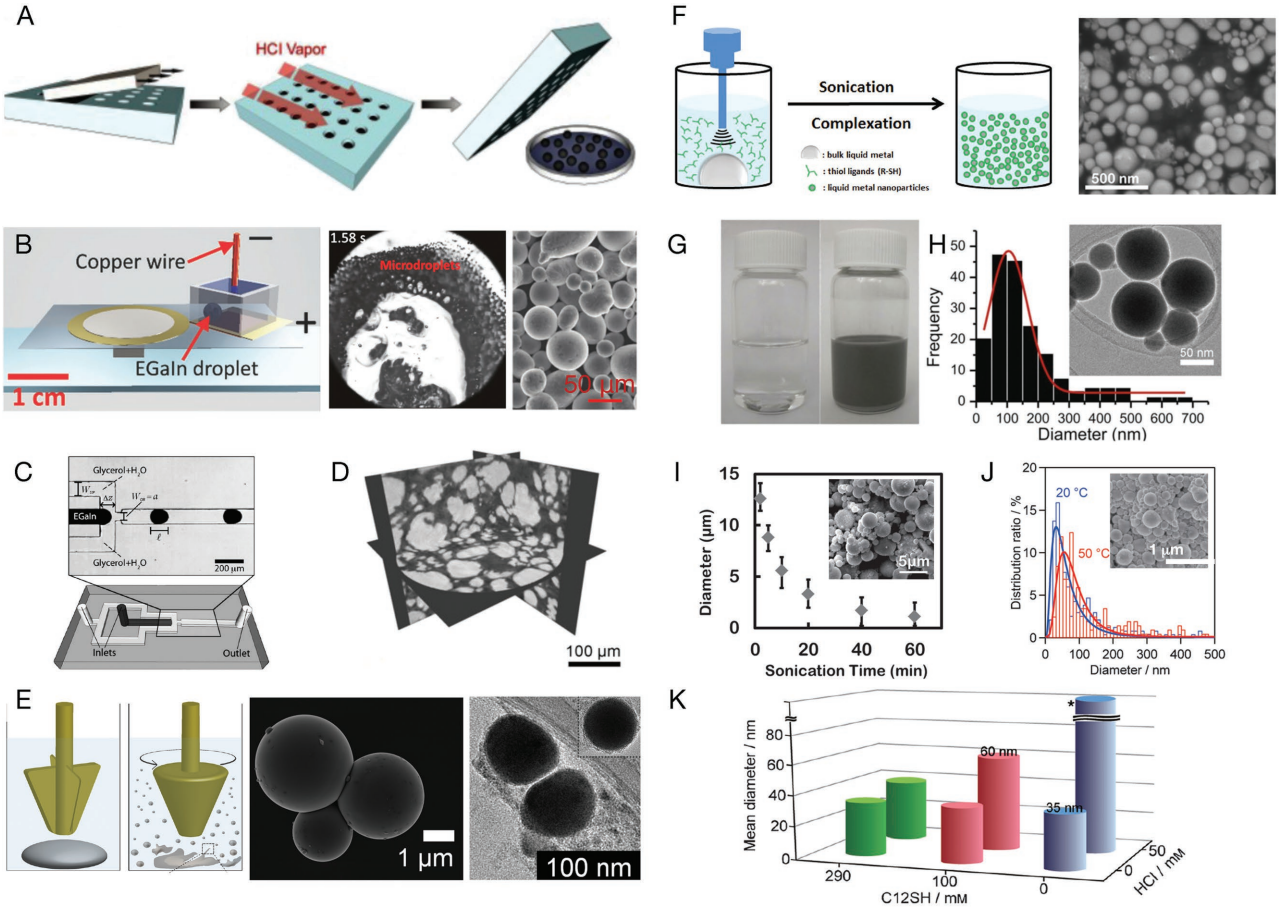

Figure 4. Demonstrating different methods of synthesizing LM droplets. A) Soft PDMS mold to create mm scale droplets. Reproduced with permission,[143] Copyright 2014, MDPI AG. B) Using acoustic wave-induced force to create microscale droplets (10–100 μm). Reproduced with permission,[144] Copyright 2016, Wiley-VCH. C) Using a microfluidic flow-focusing device to synthesize microscale droplets. Reproduced with permission,[145] Copyright 2012, Royal Society of Chemistry. D) Shear mixing can be used to create polydisperse inclusions in soft elastomer (5–50 μm). Reproduced with permission,[14] Copyright 2016, Wiey-VCH. E) Synthesis of micro- and nanoscale LM droplets. Reproduced with permission,[147] Copyright 2014, American Chemical Society. F) LM droplets can also be synthesized using ultrasonication. Reproduced with permission,[150] Copyright 2016, Wiley-VCH. Nanoscale droplets G) suspended in solution and have H) droplet diameters that range from tens to hundreds of nanometers. Reproduced with permission,[151] Copyright 2015, Wiley-VCH. I) Average droplet diameter can be controlled by sonication time (Reproduced with permission,[52] Copyright 2014, Wiley-VCH), J) temperature,[152] and K) concentrations of acid or surfactant.[152] Reproduced with permission,[152] Copyright 2015, Wiley-VCH.

further, it could help to use a core-shell model[147] to explore how the mechanics of the oxide skin may influence the effective stiffness of the composite. More generally, homogenization theories have the potential to provide predictions and insights for the mechanics of LM inclusions in elastomer,[158–160] although this still remains an area of nascent research.

Another feature of EGaIn-silicone composites that distinguishes it from other particle-filled compositions is that they exhibit relatively little mechanical hysteresis. Stress-strain curves measured during tensile loading and unloading appear to be in good agreement during cyclical mechanical tests of up to 300%. However, as with other elastomer composites, an initial stress-softening (i.e., "Mullins") effect[162,163] is measured in which the material exhibits a distinct elastic response during its first cycle of loading.[14,141] After a virgin sample is initially loaded to 200% strain, subsequent measurements of the 10% elastic modulus are in good agreement and similar to that of an unfilled elastomer. For example, the values reported in Figure 5B for the elastic modulus were taken after several loading cycles in order to eliminate this effect.[141] In order to explain the underlying cause of the Mullins effect, several theories have been postulated: (i) rupture of bonds at rubber-particle interfaces,[164] (ii) rupture of chains linking two particles,[165] (iii) slippage of molecules and bond-reformation at the surface of inclusions,[166,167] (iv) rupture of filler structure at high volume loading,[168] and (v) reduction of entanglement density.[169,170] Presently, there is no universally accepted model that provides quantitative predictions based on known physical quantities.[163] Nonetheless, these theories can potentially provide qualitative insights into the Mullins effect and other inelastic responses of fluid-filled elastomer composites during mechanical loading.

Lastly, it is expected that LMEEs and other elastomer-based gels can be engineered to exhibit significantly greater fracture toughness than homogenous elastomer. In the case of hydrogels,[171–177] fracture energies as high as ≈10 kJ m^{-2} has been reported.[72] This value is on the order of natural latex

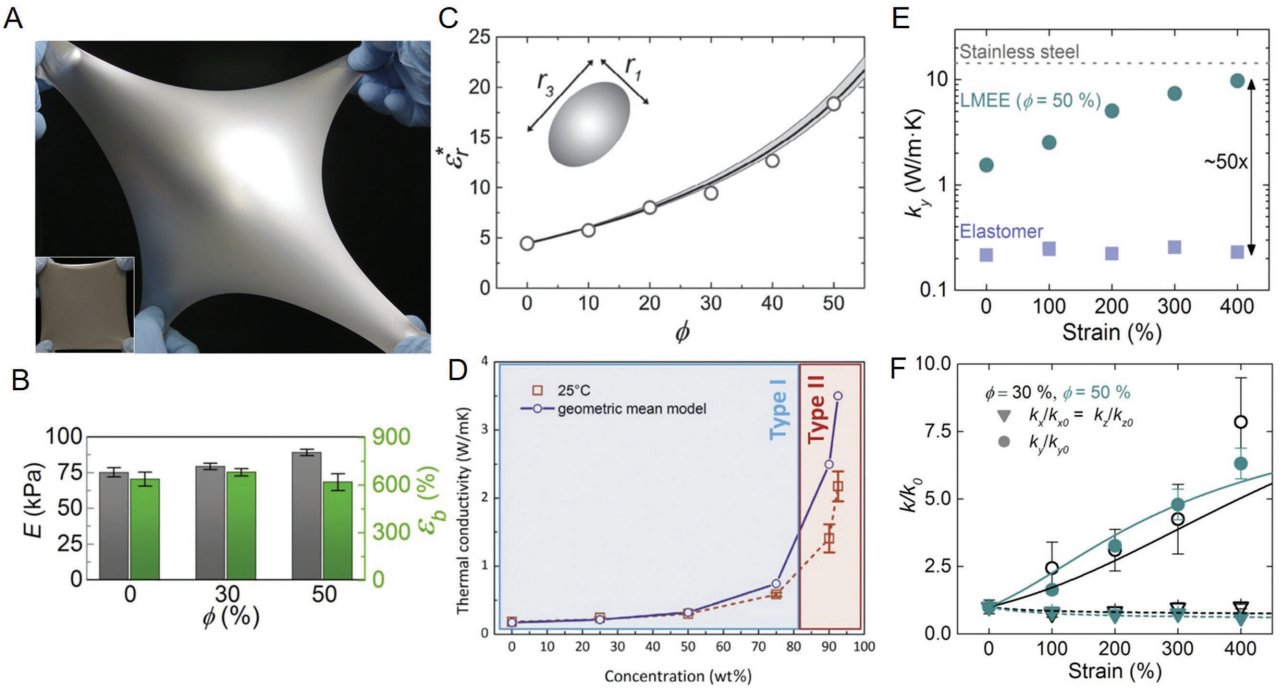

Figure 5. Characterization of LMEE: A) Image showing stretchability of LMEE with the inset of the undeformed material and B) elastic modulus and strain at break as a function of LM volume ratio. Reproduced with permission,[141] Copyright 2016, National Academy of Sciences. C) Relative permittivity of LMEE as a function of LM volume ratio: (markers) experimental measurements, (curve) theoretical predictions based on effective medium theory (EMT) adapted from Nan et al.[161] Reproduced with permission,[14] Copyright 2016, Wiley-VCH. D) Thermal conductivity of LMEE as a function of weight percentage of LM (85% weight ratio is equivalent to 50% volume ratio). Reproduced with permission,[142] Copyright 2015, Nature Publishing Group. E) Thermal conductivity in the direction of stretch as a function of strain for LMEE composite with 50% LM volume fraction and F) normalized thermal conductivity as a function of strain for 50% and 30% LM volume fraction: (markers) experimental measurements, (curve) theoretical predictions based on EMT model adapted from the Bruggeman theory. Reproduced with permission,[141] Copyright 2016, National Academy of Sciences.

rubbers[178] and over 30× greater than that of homogenous silicone. A possible contribution to this enhancement could come from crack blunting and the associated energy required to reinitiate tearing with each pore encountered along the direction of tear propagation. In the case of LMEEs, fracture energy could also be influenced by the surface tension of the LM inclusions and the resistance of their oxide skin to rupture. This represents an open topic of research and another opportunity to compare experimental measurements with theoretical predictions for heterogenous liquid-elastomer systems.

2.2. Electrical Permittivity

Fluids and elastomers embedded with a suspension of LM droplets can function like an artificial dielectric with an electrical permittivity that can exceed that of the carrier medium by up to a factor of five. Electrical insulators that have a high dielectric constant are generally attractive because of their enhanced ability to separate charge and store electrostatic energy.[133] These so-called "high-k" dielectrics can be used for transducers and sensors as well as for capacitors and other passive circuit elements. For elastomers to exhibit enhanced permittivity, they typically contain 10–30% by volume of conductive (Ag, carbon black) or insulating ($BaTiO_3$, TiO_2) filler particles.[179,180] In the case of LMEEs, similar volume fractions can lead to enhanced permittivity without causing a significant increase in elastic modulus or reduction in strain limit. For example, an EGaIn-polyurethane composite with $\phi = 0.5$ LM volume fraction exhibits a relative permittivity of $\varepsilon_r \approx 50$.[14] Moreover, its dissipation factor (loss tangent) is below 0.01 for frequencies ranging from 1 to 200 kHz. In contrast, many high-k dielectric composites with a 50% volume fraction of rigid metallic fillers become electrically lossy and unable to reliably hold electrical charge.[133,134]

Referring to Figure 5C, the experimentally measured dependency of ε_r on ϕ for an EGaIn-silicone LMEE is in good agreement with predictions based on Effective Medium Theory (EMT). The EMT model is based on a Nan formulation that accounts for composites in which inclusions have an ellipsoidal shape.[161,181] Reasonable agreement with experiment can also be obtained with a Maxwell–Garnett (M-G) formulation in which the inclusions are treated as spherical particles and ε_r is approximated by $\varepsilon_r = \varepsilon_0(1 + 2\phi)/(1 - \phi)$, where ε_0 is the permittivity of the carrier medium.[182] These models are based on a dilute suspension approximation in which the effective electrical permittivity of the binary mixture is assumed to only be governed by localized interactions between the fluidic inclusion and matrix material.

In general, effective medium predictions can be obtained by solving Maxwell's equations for the heterogeneous system. To simplify analysis, homogenization theories are used in which a

representative volumetric element of the composite is modeled as a homogenous solid with uniform bulk properties. Such representations are valid at meso- and macroscale lengths, where the dimensions of the solid are large compared to the characteristic lengths of the heterogenous features. These homogenization theories are approximate models that typically yield either upper or lower bounds to the exact solutions of the governing field equations. For problems in electro-elastostatics, such bounds have been derived by Hashin & Shtrikman[183] using variational methods.

Recently, Lopez-Pamies et al. has extended these techniques to examine electromechanical coupling in heterogeneous systems under small strains, including multi-phase compositions of fluidic inclusions in an elastic carrier medium.[158] This approach is based on an iterative homogenization theory[159,184] specialized to elastic dielectric media and can be used to recover the classical results of Hashin & Shtrikman in the case of uniform particle-particle interactions. In refs. [159] and [160], Lefèvre and Lopez-Pamies explicitly examine the mechanics, permittivity, and electrostriction of soft elastic materials embedded with liquid-like high-permittivity particles. They find that composites with larger volume fraction Φ exhibit significantly greater electrostriction but also show a significant reduction in the limiting electric field at which electromechanical instability is expected to occur.

Areas of potential future research include examination of dielectric properties at higher frequencies (i.e., MHz to THz) as well as the influence of LM inclusions on electric breakdown strength. In general, the permittivity and loss tangent of polymer-based artificial dielectrics can have a strong dependency on frequency, especially in the microwave frequency range.[185,186] The influence of composite heterogeneity and conductive inclusions on breakdown has also been studied in polymer-based artificial dielectrics. For example, the breakdown strength of a high-k Ag-epoxy composite decreases smoothly from 25 to ≈1 MV m^{-1} as the volume fraction of Ag nanoparticles increases from 0 to 25.2%.[187] Such trends are consistent with theoretical predictions based on stochastic methods, deterministic lattice models, and continuum approaches.[188] This includes computational techniques based on Monte Carlo-based simulation[189] and analytic modeling with analogies to Griffith's theory for brittle fracture.[190]

2.3. Thermal Properties

For dielectric materials where thermal transport is governed by phonons, higher thermal conductivity typically coincides with greater mechanical stiffness.[191] This thermal-mechanical tradeoff can be avoided by using LM for thermal transport and cooling.[192] One approach is to use LMEEs, in which the LM inclusions function as pathways for thermal transport without introducing mechanical rigidity. As shown in Figure 5D, Jeong et al. showed that LMEEs composed of EGaIn droplets embedded in PDMS could exhibit an order of magnitude increase in thermal conductivity compared to unfilled PDMS.[142] Bartlett et al. subsequently showed that composites with a more uniform LM dispersion could not only achieve enhanced thermal conductivity but also preserve the strain limit and elastic modulus of the base elastomer (Figure 5E).[14] Further enhancements in thermal conductivity are achieved by exploiting thermal-mechanical coupling of highly deformable LM inclusions in soft elastomers.[141] This allows for an exceptional combination of low modulus (<100 kPa) and a high thermal conductivity approaching that of metals like stainless steel and bismuth. Additionally, suspensions of micro-nano LM droplets inside silicon oil and water through sonication, have resulted in greases and emulsions with high thermal conductivity.[193,194]

The Bruggeman EMT formulation[181] can be modified to predict change in thermal conductivity as a function of uniform strain. It is assumed that all the particles start as spheres and then adopt the same mechanical strain field as the host elastomers. In order to take into account inter-particle interactions, an EMT model based on an iterative technique[195] is developed to calculate the composite thermal conductivity. This formulation yields the following implicit relationship

$$\left(\frac{k_p - k_c}{k_p - k_m}\right)\left(\frac{k_m}{k_c}\right)^L = 1 - \phi \tag{2}$$

where k_c is the composite thermal conductivity, k_p is the LM thermal conductivity, k_m is the elastomer thermal conductivity, ϕ is the LM volume ratio, and L is the depolarization factor, which depends on the strain ε.[141] As shown in Figure 5F, the increase in thermal conductivity is in good agreement with this adaptation of the Bruggeman formulation.

3. Connected LM Networks

Depending on volume fraction and spatial distribution, the embedded LM can form a connected network that supports electrical conductivity. These networks can be ordered, for example, a 3D grid or periodic lattice, or random. The latter includes gels or foams with open pores that are filled with LM.

3.1. Ordered Networks

An embedded LM network is "ordered" if the shape of the inclusions is uniform and their spacing is periodic. When connected, these inclusions form a conductive network that gives the composite an effective bulk electrical conductivity. One example is a grid-like open foam that is back-filled with LM. The mechanical integrity, elasticity, and electrical properties of such a system is governed by LM-elastomer interfacial wetting and 3D architecture. The latter is limited by available fabrication methods, which in general involves either direct elastomer 3D printing or molding techniques in which a sacrificial template/scaffold (negative) is used for casting elastomer.

Park et al. introduced a photolithography technique to produce a 3D polymer template using proximity-field nanopatterning (PnP).[2] This sacrificial template is used to cast PDMS and is removed by a water-based developer after the elastomer is cured. Scanning electron microscope images show a fairly consistent 3D grid-like elastomer microstructure (**Figure 6**A). Next,

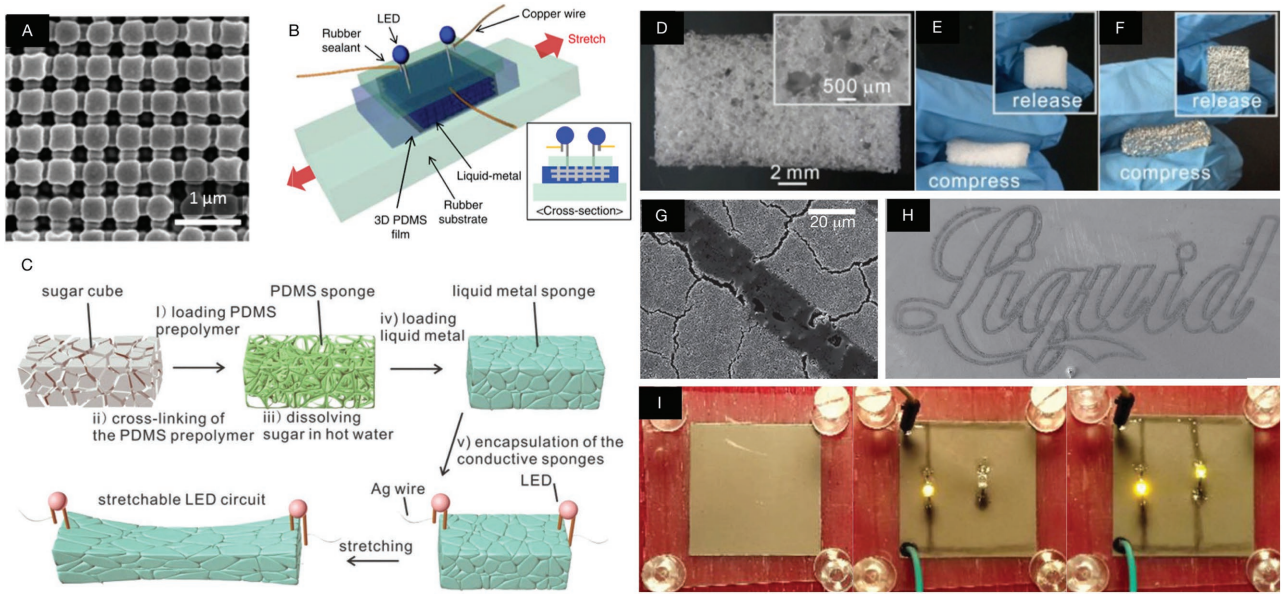

Figure 6. A) SEM image of PDMS grip produced using a 3D templating technique. B) Method for connecting LM-filled PDMS structure to an LED. Reproduced with permission,[2] Copyright 2012, Nature Publishing Group. C) Facile technique for creating LM-filled PDMS sponge. D) Unfilled PDMS sponge E) under compression. F) Galinstan-filled PDMS sponge under deformation. Reproduced with permission,[1] Copyright 2016, Royal Society of Chemistry. G) Conductive trace of ruptured EGaIn nanoparticles produced with mechanical (Reproduced with permission,[148] Copyright 2015, Wiley-VCH) and H) laser (Reproduced with permission,[151] Copyright 2015, Wiley-VCH) sintering. I) Conductive traces in LMEE produced with applied surface pressure. Reproduced with permission,[140] Copyright 2015, Wiley-VCH.

the PDMS is vacuum injected with EGaIn, creating conductive interconnected 3D channels throughout. This technique has been shown to support a simple LED circuit (Figure 6B) with a conductivity of $\approx 2.4 \times 10^6$ S m^{-1} and minimal degradation over many loading cycles.

3.2. Random Networks

An open foam elastomer can also be produced by filling sugar cubes with a PDMS prepolymer and then dissolving away the sugar after the elastomer cures. This results in a sponge with random pores that can then be filled with LM (Figure 6C,D).[1] The presence of LM does not significantly interfere with the ability to deform the PDMS sponge under light compression (Figure 6E,F). Depending on the sponge porosity, the effective volumetric conductivity of the bulk system can be as high as 1.6×10^6 S m^{-1}, similar to that of the ordered network.[2] The advantage of this facile technique is that it eliminates the need for PnP-based templating or other specialized techniques for 3D elastomer patterning.

Random LM networks in an open foam matrix can also be accomplished with "mechanical sintering" techniques that involve the application of highly localized pressure to an LMEE composite. In the case of EGaIn nanodroplets produced with ultrasonication, it has been previously shown that high pressure can rupture the Ga_2O_3 skin and cause droplets to coalesce into conductive traces (Figure 6G).[148] Alternatively, droplet rupture and coalescence can be induced through laser-based sintering using a CO_2 laser engraver (Figure 6H).[151] For certain LMEE compositions, mechanically sintering can be used to permanently transform the composite from an electrical insulator into a conductor. It has been shown that stiffer LMEE composites composed of highly cross-linked PDMS (Sylgard 184; Dow-Corning) with 50% (by vol.) loading EGaIn can exhibit permanent electrical conductivity (10^4 S m^{-1}) when subject to intense pressure with a roller or ball-point pen (Figure 6I).[140] Moreover, electrical resistance of the trace does not change significantly when stretched to 125% strain. This apparent departure from Ohm's law is likely related to the governing role of contact resistance between LM droplets, which is not expected to change significantly with stretch.

In general, electrical conductivity can be accomplished with percolative networks in which the fluid exhibits long-range connectivity throughout the volume of the composite. For a liquid dispersion with statistically uniform spatial distribution, percolation typically requires a high volume fraction ϕ such that the inclusions are packed sufficiently tight and in physical contact.[196] Even in the absence of direct contact, electrical connectivity is still possible through electrical tunneling over interfacial gaps of $\approx$0.1–1 nm.[197] In the special case of embedded spherical inclusions with fixed diameter and periodic spatial distribution, the percolation threshold ϕ' can be determined for a variety of lattice geometries, including cubic, body-centered, and face-centered.[198–200] However, electrical conductivity may not be significant even when ϕ' is exceeded. This could be on account of the insulating Ga_2O_3 skin covering the LM droplets[122,124] or conformal wetting of the elastomer.

4. Connected LMPA Networks

As with LM-based composites, connected LMPA networks embedded in elastomer can also be categorized into ordered

or random. In both cases, the LMPA-elastomer system can be engineered to function as a rigidity-tuning composite that undergoes dramatic change in stiffness when the embedded alloy melts. Such phase change can be controlled with external heating or by internal Joule heating with electrical current. Stiffness tuning can also be accomplished with shape memory alloys,[201] shape memory polymers,[131,202] thermoplastics,[203–205] and a variety of other techniques.[206,207] However, LMPAs remain attractive due to the dramatic change in mechanical compliance – from a rigid solid (modulus ≈10 GPa) to fluidic.

4.1. Ordered Networks

Schubert et al.[21] introduced a variable stiffness composite in which PDMS was embedded with a serpentine channel of Field's metal (**Figure 7**A). As in conventional soft microfluidics, the channels were cast using a micromachined mold produced with clean-room lithography. Applying electrical current to the LMPA trace led to Joule heating and an increase in temperature. When the embedded Field's metal heated above its melting point, the flexural rigidity of the composite reduced by a factor of 25 (Figure 7B,C). As with other approaches to rigidity tuning with Field's metal, the activation can be rapid (<1s) but deactivation is slow (≈1 min) since it requires the alloy to cool to below its melting temperature.

Another architecture for LMPA-based rigidity-tuning was recently introduced by Tonazzini et al.[128] In their design, an LMPA core is embedded inside silicon elastomer along with a conductive wire, which is used as a heater (Figure 7D). Use of an embedded heater is also adopted by Shan et al., who demonstrated that a strip of Field's metal in a soft polyacrylate can be melted with an embedded LM heater.[131] The activation rate (≈30s) of the variable stiffness fiber is slower than with direct Joule heating since it is controlled by thermal convection.[128,208]

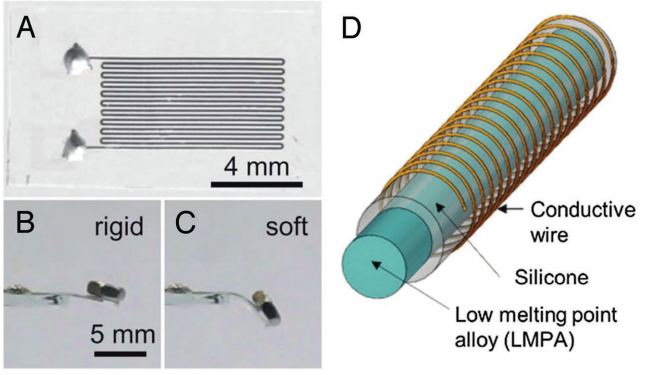

Figure 7. A) Rigidity-tuning material composed of a PDMS film embedded with a serpentine microchannel filled with Field's metal.[21] B) At room temperature, the material is effectively rigid and load bearing. C) When electrical current is delivered, the metal trace melts and the flexural rigidity of the composite decreases by a factor of 25. Reproduced with permission, Copyright 2013, Royal Society of Chemistry. D) Schematic of variable stiffness fiber (VSF), using LMPA as the core material. The alloy is encapsulated with a PDMS shell that is wrapped in a conductive wire for delivering heat. Reproduced with permission,[128] Copyright 2016, Wiley-VCH.

However, the rigidity change is significantly large (>700×) and the composite can exhibit self-healing through a process that involves cyclical melting and solidification. Fusible low-melting-point alloys can also be combined with dielectric elastomer actuators[209] or shape memory alloys[210] to create actuators that independently tune their shape and stiffness.

4.2. Random Porosity

Using an approach similar to that by Liang et al. for an LM-filled PDMS sponge,[1] Van Meerbeek et al. created a novel LMPA-elastomer composite[53] with random porosity. A porous elastomer foam (**Figure 8**A) is filled with melted Field's metal (Figure 8B) using vacuum pressure. Next, the alloy is allowed to cool to room temperature and solidify. As with other LMPA-elastomer systems, the foam exhibits rigidity tuning (Figure 8C,D), shape memory, and self healing properties. The composite shows stiffness change of 18× in tension and 30× in compression. By deforming the foam and freezing the LMPA, Van Meerbeek et al.[53] could create elongated and twisted shapes. After raising the temperature and melting the LMPA, the elastomer is allowed to release stored elastic energy and the foam springs back to its natural shape.

Such LMPA-elastomer composites can be used for on-demand changes in structural load-bearing. In a bioinspired system, they could potentially function as a tunable skeleton or exoskeleton that matches some of the properties of catch connective tissue[211,212] or a muscular hydrostat.[213] They could also be integrated into a soft robotic actuator to produce an

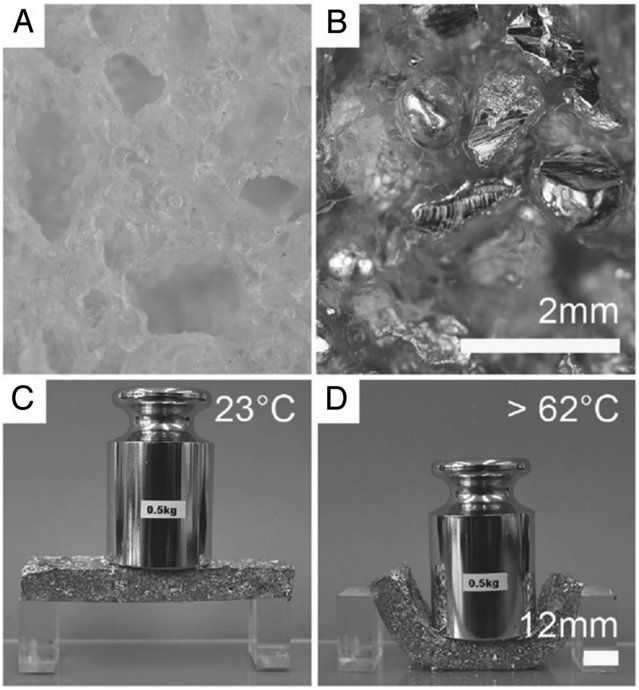

Figure 8. A) Soft silicone foam and B) bicontinuous LMPA foam for tunable elastic rigidity. C) LMPA-elastomer composite under a 500 g load near room temperature and D) when heated above the melting point of the alloy. Reproduced with permission,[53] Copyright 2016, Wiley-VCH.

artificial muscle capable of independent control of stiffness and shape. Additionally, the range of stiffness change can be tailored by modifying the foam microstructure or varying the choice of LMPA.[214–216] Van Meerbeek et al.[53] used an external heater to initiate the melting process, however embedding soft heating elements or running electrical current directly through the alloy can improve portability and reduce activation time.

5. Conclusions and Outlook

In this progress report, we presented an overview of efforts to engineer soft multifunctional systems with LM or LMPAs. When incorporated into an elastomer, these alloys can either preserve the elasticity of the surrounding medium or be used to actively tune its mechanical properties. In most cases, the LM or LMPA dispersion has a random but statistically uniform spatial distribution that results in a heterogenous composite with effective bulk properties. This is distinct from LM microfluidics, printed circuits, and other deterministically patterned implementations.

The micro- or mesoscale structure of these LMPA and LM-embedded elastomer (LMEE) composites can be engineered using a variety of synthesis techniques. Depending on their structure and composition, they can exhibit combinations of electrical, thermal, and mechanical properties that are not typically observed in other soft material systems. This includes rubber-like elasticity combined with metal-like thermal or electrical conductivity and the ability to rapidly and reversibly change rigidity through thermal or electrical stimulation. Some of the bulk properties of these composites can be understood using effective medium approximations and modifications to classical homogenization theories. Both theory and experiment suggest that certain emergent properties can arise in which the composite exhibits features that are not observed with the bulk constituents. This includes electrical and thermal anisotropies and the possibility for dramatic enhancements in fracture toughness. In the case of LMEE composites that become conductive through mechanical sintering, another emergent feature is the ability to maintain a fixed electrical resistance during stretch.

Further progress with this novel class of soft multifunctional materials will continue to build on practices and fundamental insights from interface and colloid science, microfluidics, and condensed soft-matter physics. There is still much to learn about materials integration, including the synthesis of LM and LMPA nanoparticles and their dispersion in elastic materials. While effective medium approximations have been useful for modeling some bulk composite properties (e.g., dielectric constant, thermal conductivity), additional work is required to establish theories that can fully explain the mechanical, electrical, and thermal features of these systems and their stress-induced responses. This is particularly true for understanding variations in fracture energy and electric breakdown, which have yet to be adequately studied. Progress in analytic and computational modeling will help inform materials design and could lead to further enhancements or new functionalities. Such improvements have the potential to advance emerging fields like soft robotics and wearable computing by enabling soft materials to exhibit an even greater range of properties without sacrificing their natural mechanical compliance. Note: When initially published online, the graphic for Figure 3 had been set as Figure 4 and the graphic for Figure 4 set as Figure 3. This was corrected on July 13, 2017.

Keywords

dielectric elastomers, eutectic gallium-indium, low-melting-point alloys, soft multifunctional materials, stretchable electronics

Received: November 6, 2016
Revised: February 19, 2017
Published online: April 20, 2017

[1] S. Liang, Y. Li, Y. Chen, J. Yang, T. Zhu, D. Zhu, C. He, Y. Liu, S. Handschuh-Wang, X. Zhou, *J. Mater. Chem. C* **2016**, *5*, 1586.
[2] J. Park, S. Wang, M. Li, C. Ahn, J. K. Hyun, D. S. Kim, D. K. Kim, J. A. Rogers, Y. Huang, S. Jeon, *Nat. Commun.* **2012**, *3*, 916.
[3] H. Stoyanov, M. Kollosche, S. Risse, D. N. McCarthy, G. Kofod, *Soft Matter* **2011**, *7*, 194.
[4] J. A. Rogers, T. Someya, Y. Huang, *Science* **2010**, *327*, 1603.
[5] M. L. Hammock, A. Chortos, B. C. K. Tee, J. B. H. Tok, Z. Bao, *Adv. Mater.* **2013**, *25*, 5997.
[6] M. A. Unger, H.-P. Chou, T. Thorsen, A. Scherer, S. R. Quake, *Science* **2000**, *288*, 113.
[7] J. C. McDonald, G. M. Whitesides, *Acc. Chem. Res.* **2002**, *35*, 491.
[8] A. C. Siegel, D. A. Bruzewicz, D. B. Weibel, G. M. Whitesides, *Adv. Mater.* **2007**, *19*, 727.
[9] Y. L. Park, B. R. Chen, R. J. Wood, *IEEE Sens. J.* **2012**, *12*, 2711.
[10] J. W. Boley, E. L. White, G. T. C. Chiu, R. K. Kramer, *Adv. Funct. Mater.* **2014**, *24*, 3501.
[11] B. A. Gozen, A. Tabatabai, O. B. Ozdoganlar, C. Majidi, *Adv. Mater.* **2014**, *26*, 5211.
[12] M. R. Khan, C. B. Eaker, E. F. Bowden, M. D. Dickey, *Proc. Natl. Acad. Sci. USA* **2014**, *111*, 14047.
[13] T. Hutter, W. A. C. Bauer, S. R. Elliott, W. T. S. Huck, *Adv. Funct. Mater.* **2012**, *22*, 2624.
[14] M. D. Bartlett, A. Fassler, N. Kazem, E. J. Markvicka, P. Mandal, C. Majidi, *Adv. Mater.* **2016**, *28*, 3726.
[15] J. N. Hohman, M. Kim, G. A. Wadsworth, H. R. Bednar, J. Jiang, M. A. LeThai, P. S. Weiss, *Nano Lett.* **2011**, *11*, 5104.
[16] J. H. Koo, *Polymer Nanocomposites*, McGraw-Hill, New York, **2006**.
[17] M. Maiti, M. Bhattacharya, A. K. Bhowmick, *Rubber Chem. Technol.* **2008**, *81*, 384.
[18] P.-C. Ma, N. A. Siddiqui, G. Marom, J.-K. Kim, *Composites, Part A* **2010**, *41*, 1345.
[19] A. K. Gaharwar, N. A. Peppas, A. Khademhosseini, *Biotechnol. Bioeng.* **2014**, *111*, 441.
[20] M. D. Dickey, R. C. Chiechi, R. J. Larsen, E. A. Weiss, D. A. Weitz, G. M. Whitesides, *Adv. Funct. Mater.* **2008**, *18*, 1097.
[21] B. E. Schubert, D. Floreano, *RSC Adv.* **2013**, *3*, 24671.
[22] J. C. Halbur, R. P. Padbury, J. S. Jur, *J. Vac. Sci. Technol., A* **2016**, *34*, 031402.
[23] S. W. Thomas, G. D. Joly, T. M. Swager, *Chem. Rev.* **2007**, *107*, 1339.
[24] J. Pecher, S. Mecking, *Chem. Rev.* **2010**, *110*, 6260.
[25] S. Günes, H. Neugebauer, N. Sariciftci, *Chem. Rev.* **2007**, *107*, 1324.
[26] A. C. Grimsdale, K. L. Chan, R. E. Martin, P. G. Jokisz, A. B. Holmes, *Chem. Rev.* **2009**, *109*, 897.
[27] C. A. Junwu, C. Yong, *Acc. Chem. Res.* **2009**, *42*, 1709.
[28] G.-H. Kim, D. Lee, A. Shanker, L. Shao, M. S. Kwon, D. Gidley, J. Kim, K. P. Pipe, *Nat. Mater.* **2015**, *14*, 295.

[29] Y. Xia, Y. Lu, *Compos. Sci. Technol.* **2008**, *68*, 1471.
[30] X. Z. Niu, S. L. Peng, L. Y. Liu, W. J. Wen, P. Sheng, *Adv. Mater.* **2007**, *19*, 2682.
[31] Z. Fan, J. C. Ho, T. Takahashi, R. Yerushalmi, K. Takei, A. C. Ford, Y. L. Chueh, A. Javey, *Adv. Mater.* **2009**, *21*, 3730.
[32] Y. Sun, J. A. Rogers, *Adv. Mater.* **2007**, *19*, 1897.
[33] W. Bauhofer, J. Z. Kovacs, *Compos. Sci. Technol.* **2009**, *69*, 1486.
[34] A. Khosla, B. L. Gray, *Mater. Lett.* **2009**, *63*, 1203.
[35] P. Lee, J. Lee, H. Lee, J. Yeo, S. Hong, K. H. Nam, D. Lee, S. S. Lee, S. H. Ko, *Adv. Mater.* **2012**, *24*, 3326.
[36] M. B. Bryning, D. E. Milkie, M. F. Islam, L. A. Hough, J. M. Kikkawa, A. G. Yodh, *Adv. Mater.* **2007**, *19*, 661.
[37] S. M. Jung, H. Y. Jung, M. S. Dresselhaus, Y. J. Jung, J. Kong, *Sci. Rep.* **2012**, *2*, 849.
[38] N. Kazem, C. Majidi, C. E. Maloney, *Soft Matter* **2015**, *11*, 7877.
[39] D.-Y. Khang, H. Jiang, Y. Huang, J. A. Rogers, *Science* **2006**, *311*, 208.
[40] D.-H. Kim, J.-H. Ahn, W. M. Choi, H.-S. Kim, T.-H. Kim, J. Song, Y. Y. Huang, Z. Liu, C. Lu, J. A. Rogers, *Science* **2008**, *320*, 507.
[41] H. C. Ko, M. P. Stoykovich, J. Song, V. Malyarchuk, W. M. Choi, C. J. Yu, J. B. Geddes 3rd, J. Xiao, S. Wang, Y. Huang, J. A. Rogers, *Nature* **2008**, *454*, 748.
[42] H. C. Ko, G. Shin, S. Wang, M. P. Stoykovich, J. W. Lee, D. H. Kim, J. S. Ha, Y. Huang, K. C. Hwang, J. A. Rogers, *Small* **2009**, *5*, 2703.
[43] S.-I. Park, Y. Xiong, R.-H. Kim, P. Elvikis, M. Meitl, D.-H. Kim, J. Wu, J. Yoon, C.-J. Yu, Z. Liu, Y. Huang, K.-c. Hwang, P. Ferreira, X. Li, K. Choquette, J. A. Rogers, *Science* **2009**, *325*, 977.
[44] D.-H. Kim, J. Viventi, J. J. Amsden, J. Xiao, L. Vigeland, Y.-S. Kim, J. A. Blanco, B. Panilaitis, E. S. Frechette, D. Contreras, D. L. Kaplan, F. G. Omenetto, Y. Huang, K.-C. Hwang, M. R. Zakin, B. Litt, J. A. Rogers, *Nat. Mater.* **2010**, *9*, 511.
[45] R.-H. Kim, D.-H. Kim, J. Xiao, B. H. Kim, S.-I. Park, B. Panilaitis, R. Ghaffari, J. Yao, M. Li, Z. Liu, V. Malyarchuk, D. G. Kim, A.-P. Le, R. G. Nuzzo, D. L. Kaplan, F. G. Omenetto, Y. Huang, Z. Kang, J. A. Rogers, *Nat. Mater.* **2010**, *9*, 929.
[46] D.-H. Kim, N. Lu, R. Ghaffari, Y.-S. Kim, S. P. Lee, L. Xu, J. Wu, R.-H. Kim, J. Song, Z. Liu, J. Viventi, B. de Graff, B. Elolampi, M. Mansour, M. J. Slepian, S. Hwang, J. D. Moss, S.-M. Won, Y. Huang, B. Litt, J. A. Rogers, *Nat. Mater.* **2011**, *10*, 316.
[47] H. Keum, M. Mccormick, P. Liu, Y.-W. Zhang, F. G. Omenetto, *Science* **2011**, *333*, 838.
[48] I. Jung, J. Xiao, V. Malyarchuk, C. Lu, M. Li, Z. Liu, J. Yoon, Y. Huang, J. A. Rogers, *Proc. Natl. Acad. Sci. USA* **2011**, *108*, 1788.
[49] S. Xu, Y. Zhang, J. Cho, J. Lee, X. Huang, L. Jia, J. a. Fan, Y. Su, J. Su, H. Zhang, H. Cheng, B. Lu, C. Yu, C. Chuang, T.-I. Kim, T. Song, K. Shigeta, S. Kang, C. Dagdeviren, I. Petrov, P. V. Braun, Y. Huang, U. Paik, J. A. Rogers, *Nat. Commun.* **2013**, *4*, 1543.
[50] R. C. Chiechi, E. A. Weiss, M. D. Dickey, G. M. Whitesides, *Angew. Chem.* **2008**, *120*, 148.
[51] A. Fassler, C. Majidi, *Smart Mater. Struct.* **2013**, *22*, 055023.
[52] W. Zhang, J. Z. Ou, S. Y. Tang, V. Sivan, D. D. Yao, K. Latham, K. Khoshmanesh, A. Mitchell, A. P. O'Mullane, K. Kalantar-Zadeh, *Adv. Funct. Mater.* **2014**, *24*, 3799.
[53] I. M. Van Meerbeek, B. C. Mac Murray, J. W. Kim, S. S. Robinson, P. X. Zou, M. N. Silberstein, R. F. Shepherd, *Adv. Mater.* **2016**, 2801.
[54] S. Cheng, Z. Wu, *Lab Chip* **2010**, *10*, 3227.
[55] H. J. Koo, J. H. So, M. D. Dickey, O. D. Velev, *Adv. Mater.* **2011**, *23*, 3559.
[56] S. H. Jeong, A. Hagman, K. Hjort, M. Jobs, J. Sundqvist, Z. Wu, *Lab Chip* **2012**, *12*, 4657.
[57] A. Fassler, C. Majidi, *Lab Chip* **2013**, *13*, 4442.
[58] M. D. Dickey, *ACS Appl. Mater. Interfaces* **2014**, *6*, 18369.
[59] C. Koo, B. E. LeBlanc, M. Kelley, H. E. Fitzgerald, G. H. Huff, A. Han, *J. Microelectromech. Syst.* **2014**, *24*, 1069.
[60] I. D. Joshipura, H. R. Ayers, C. Majidi, M. D. Dickey, *J. Mater. Chem. C* **2015**, *3*, 3834.
[61] S. W. Jin, J. Park, S. Y. Hong, H. Park, Y. R. Jeong, J. Park, S.-S. Lee, J. S. Ha, *Sci. Rep.* **2015**, *5*, 11695.
[62] M. Wang, C. Trlica, M. R. Khan, M. D. Dickey, J. J. Adams, *J. Appl. Phys.* **2015**, *117*.
[63] C. B. Eaker, M. D. Dickey, *Appl. Phys. Rev.* **2016**, *3*, 031103.
[64] M. Khondoker, D. Sameoto, *Smart Mater. Struct.* **2016**, *25*, 093001.
[65] M. U. Memon, K. Ling, Y. Seo, S. Lim, *J. Electromagn. Waves Appl.* **2015**, *29*, 2207.
[66] J.-B. Chossat, Y. Tao, V. Duchaine, Y.-L. Park, *IEEE Int. Conf. Robotics and Automation*(ICRA), Seattle, WA, USA **2015**, 2568.
[67] M. Gao, L. Gui, *Lab Chip* **2014**, *14*, 1866.
[68] Y. Menguc, Y.-L. Park, H. Pei, D. Vogt, P. M. Aubin, E. Winchell, L. Fluke, L. Stirling, R. J. Wood, C. J. Walsh, *Int. J. Rob. Res.* **2014**, *33*, 1748.
[69] F. L. Hammond, R. K. Kramer, Q. Wan, R. D. Howe, R. J. Wood, F. L. H. III, R. K. Kramer, Q. Wan, R. D. Howe, R. J. Wood, *IEEE Int. Conf. Intell. Rob. Syst. (IROS)* **2014**, *14*, 1443.
[70] D. M. Vogt, R. J. Wood, *IEEE Sens. Conf.*, Valencia, Spain **2014**, 1631.
[71] C. Keplinger, J.-Y. Y. Sun, C. C. Foo, P. Rothemund, G. M. Whitesides, Z. Suo, *Science* **2013**, *341*, 984.
[72] J.-Y. Sun, X. Zhao, W. R. K. Illeperuma, O. Chaudhuri, K. H. Oh, D. J. Mooney, J. J. Vlassak, Z. Suo, *Nature* **2012**, *489*, 133.
[73] Y. Shi, L. Pan, B. Liu, Y. Wang, Y. Cui, Z. Bao, G. Yu, *J. Mater. Chem. A* **2014**, *2*, 6086.
[74] J. S. Noh, *Polymers* **2016**, *8*, 123.
[75] J. Park, I. You, S. Shin, U. Jeong, *ChemPhysChem* **2015**, *16*, 1155.
[76] S. Liu, X. Sun, O. J. Hildreth, K. Rykaczewski, *Lab Chip* **2015**, *15*, 1376.
[77] Y. L. Han, H. Liu, C. Ouyang, T. J. Lu, F. Xu, *Sci. Rep.* **2015**, *5*, 11488.
[78] D. P. Parekh, C. Ladd, L. Panich, K. Moussa, M. D. Dickey, *Lab Chip* **2016**, *16*, 1812.
[79] S. Kim, J. Lee, B. Choi, *IEEE Sens. J.* **2015**, *15*, 6077.
[80] R. A. Awang, T. Baum, M. Nasabi, S. Sriram, W. S. T. Rowe, *Smart Mater. Struct.* **2016**, *25*, 075023.
[81] A. P. Saghati, J. S. Batra, J. Kameoka, K. Entesari, *IEEE Antennas Wireless Propag. Lett.* **2016**, *15*, 122.
[82] A. P. Saghati, J. S. Batra, J. Kameoka, K. Entesari, *IEEE Trans. Microwave Theory Tech.* **2015**, *63*, 2515.
[83] K. Ling, H. K. Kim, M. Yoo, S. Lim, *Sensors* **2015**, *15*, 28154.
[84] D. Kim, J. H. Yoo, J.-B. Lee, *J. Micromech. Microeng.* **2016**, *26*, 045004.
[85] B. L. Cumby, G. J. Hayes, M. D. Dickey, R. S. Justice, C. E. Tabor, J. C. Heikenfeld, *Appl. Phys. Lett.* **2012**, *101*, 1.
[86] R. C. Gough, A. M. Morishita, J. H. Dang, W. Hu, W. A. Shiroma, A. T. Ohta, *IEEE Access* **2014**, *2*, 874.
[87] Z. Wu, K. Hjort, S. H. Jeong, *Proc. IEEE* **2015**, *103*, 1211.
[88] A. P. Saghati, J. S. Batra, J. Kameoka, K. Entesari, *IEEE Trans. Antennas Propag.* **2015**, *63*, 3798.
[89] R. C. Ordonez, C. K. Hayashi, C. M. Torres, N. Hafner, J. R. Adleman, N. M. Acosta, J. Melcher, N. M. Kamin, D. Garmire, *IEEE Trans. Electron Devices* **2016**, *63*, 4018.
[90] F. Ongul, S. Yuksel, S. Bozar, G. Cakmak, H. Guney, D. Egbe, S. Gunes, *J. Phys. D: Appl. Phys.* **2015**, *48*, 175102.
[91] J. Wissman, L. Finkenauer, L. Deseri, C. Majidi, *J. Appl. Phys.* **2014**, *116*, 144905.
[92] K. Ling, K. Kim, S. Lim, *Opt. Express* **2015**, *23*, 21375.
[93] J. Wang, S. Liu, S. Guruswamy, A. Nahata, *Opt. Express* **2014**, *22*, 4065.
[94] H. K. Kim, D. Lee, S. Lim, *Sci. Rep.* **2016**, *6*, 31823.
[95] J. Tang, J. Wang, J. Liu, Y. Zhou, *Appl. Phys. Lett.* **2016**, *108*.
[96] J. Y. Zhu, S. Y. Tang, K. Khoshmanesh, K. Ghorbani, *ACS Appl. Mater. Interfaces* **2016**, *8*, 2173.

[97] A. Zavabeti, T. Daeneke, A. F. Chrimes, A. P. O'Mullane, J. Zhen Ou, A. Mitchell, K. Khoshmanesh, K. Kalantar-zadeh, *Nat. Commun.* **2016**, *7*, 12402.
[98] M. Mohammed, R. Sundaresan, M. D. Dickey, *ACS Appl. Mater. Interfaces* **2015**, *7*, 23163.
[99] S. Y. Tang, J. Zhu, V. Sivan, B. Gol, R. Soffe, W. Zhang, A. Mitchell, K. Khoshmanesh, *Adv. Funct. Mater.* **2015**, *25*, 4445.
[100] L. Wang, J. Liu, *Proc. R. Soc. A* **2015**, *471*, 20150177.
[101] J. Wang, K. Appusamy, S. Guruswamy, A. Nahata, *Sci. Rep.* **2015**, *5*, 8637.
[102] M. R. Khan, C. Trlica, M. D. Dickey, *Adv. Funct. Mater.* **2015**, *25*, 671.
[103] S.-Y. Tang, Y. Lin, I. D. Joshipura, K. Khoshmanesh, M. D. Dickey, *Lab Chip* **2015**, *15*, 3905.
[104] E. Mitraka, L. Kergoat, Z. U. Khan, S. Fabiano, O. Douhéret, P. Leclère, M. Nilsson, P. A. Ersman, G. Gustafsson, R. Lazzaroni, M. Berggren, X. Crispin, *J. Mater. Chem. C* **2015**, *3*, 7604.
[105] J. Zhang, Y. Yao, L. Sheng, J. Liu, *Adv. Mater.* **2015**, *27*, 2648.
[106] W. Q. Fang, Z. Z. He, J. Liu, *Appl. Phys. Lett.* **2014**, *105*, 18.
[107] K. S. Wimbush, R. M. Fratila, D. Wang, D. Qi, C. Liang, L. Yuan, N. Yakovlev, K. P. Loh, D. N. Reinhoudt, A. H. Velders, C. A. Nijhuis, *Nanoscale* **2014**, *6*, 11246.
[108] A. F. Chrimes, K. J. Berean, A. Mitchell, G. Rosengarten, K. Kalantar-Zadeh, *ACS Appl. Mater. Interfaces* **2016**, *8*, 3833.
[109] M. Dickey, C. Eaker, M. R. Kahn, *J. Visualized Exp.* **2016**, *107*, e53567.
[110] G. Li, M. Parmar, D. Kim, J.-B. Lee, D.-W. Lee, *Lab Chip* **2014**, *14*, 200.
[111] D. Kim, Y. Lee, D. W. Lee, W. Choi, K. Yoo, J. B. Lee, *Sens. Actuators, B* **2015**, *207*, 199.
[112] B. Kim, J. Jang, I. You, J. Park, S. Shin, G. Jeon, J. K. Kim, U. Jeong, *ACS Appl. Mater. Interfaces* **2015**, *7*, 7920.
[113] G. Li, M. Parmar, D.-W. Lee, *Lab Chip* **2015**, *15*, 766.
[114] M. R. Khan, C. Trlica, J.-H. So, M. Valeri, M. D. Dickey, *ACS Appl. Mater. Interfaces* **2014**, *6*, 22467.
[115] M. Dickey, *Adv. Mater.* **2017**, in press.
[116] S. Cheng, Z. Wu, *Lab Chip* **2012**, *12*, 2782.
[117] S. Yu, M. Kaviany, *J. Chem. Phys.* **2014**, *140*, 064303.
[118] Y. Plevachuk, V. Sklyarchuk, S. Eckert, G. Gerbeth, R. Novakovic, *J. Chem. Eng. Data* **2014**, *59*, 757.
[119] Y. Plevachuk, V. Sklyarchuk, N. Shevchenko, S. Eckert, *Int. J. Mater. Res.* **2015**, *106*, 66.
[120] J. N. Koster, *Cryst. Res. Technol.* **1999**, *34*, 1129.
[121] Y. Lu, Q. Hu, Y. Lin, D. B. Pacardo, C. Wang, W. Sun, F. S. Ligler, M. D. Dickey, Z. Gu, *Nat. Commun.* **2015**, *6*, 10066.
[122] T. Liu, P. Sen, C. J. Kim, *J. Microelectromech. Syst.* **2012**, *21*, 443.
[123] M. J. Regan, H. Tostmann, P. S. Pershan, O. M. Magnussen, E. Dimasi, B. M. Ocko, M. Deutsch, *Phys. Rev. B* **1997**, *55*, 786.
[124] L. Cademartiri, M. M. Thuo, C. A. Nijhuis, W. F. Reus, S. Tricard, J. R. Barber, R. N. S. Sodhi, P. Brodersen, C. Kim, R. C. Chiechi, G. M. Whitesides, *J. Phys. Chem. C* **2012**, *116*, 10848.
[125] R. J. Larsen, M. D. Dickey, G. M. Whitesides, D. A. Weitz, *J. Rheol.* **2009**, *53*, 1305.
[126] S. Liu, X. Sun, N. Kemme, V. G. Damle, C. Schott, M. Herrmann, K. Rykaczewski, *Microfluid. Nanofluid.* **2016**, *20*, 1.
[127] A. C. Siegel, S. S. Shevkoplyas, D. B. Weibel, D. A. Bruzewicz, A. W. Martinez, G. M. Whitesides, *Angew. Chem. Int. Ed.* **2006**, *45*, 6877.
[128] A. Tonazzini, S. Mintchev, B. Schubert, B. Mazzolai, J. Shintake, D. Floreano, *Adv. Mater.* **2016**, *28*, 10142.
[129] V. Arabagi, O. Felfoul, A. Gosline, R. Wood, P. Dupont, *IEEE Sens. J.* **2015**, *16*, 1294.
[130] J. C. Lötters, W. Olthuis, P. H. Veltink, P. Bergveld, *J. Micromech. Microeng.* **1999**, *7*, 145.
[131] W. Shan, T. Lu, C. Majidi, *Smart Mater. Struct.* **2013**, *22*, 085005.
[132] S. Zhu, J. H. So, R. Mays, S. Desai, W. R. Barnes, B. Pourdeyhimi, M. D. Dickey, *Adv. Funct. Mater.* **2013**, *23*, 2308.
[133] Z. M. Dang, J. K. Yuan, J. W. Zha, T. Zhou, S. T. Li, G. H. Hu, *Prog. Mater. Sci.* **2012**, *57*, 660.
[134] J. Lu, C. Wong, *IEEE Trans. Dielectr. Electr. Insul.* **2008**, *15*, 1322.
[135] M. Park, J. Park, U. Jeong, *Nano Today* **2014**, *9*, 244.
[136] H. Stoyanov, M. Kollosche, S. Risse, R. Waché, G. Kofod, *Adv. Mater.* **2013**, *25*, 578.
[137] J. Cho, M. Joshi, C. Sun, *Compos. Sci. Technol.* **2006**, *66*, 1941.
[138] L. Bokobza, C. Belin, *J. Appl. Polym. Sci.* **2007**, *105*, 2054.
[139] S.-Y. Fu, X.-Q. Feng, B. Lauke, Y.-W. Mai, *Composites, Part B* **2008**, *39*, 933.
[140] A. Fassler, C. Majidi, *Adv. Mater.* **2015**, *27*, 1928.
[141] M. D. Bartlett, N. Kazem, M. J. Powell-Palm, X. Huang, W. Sun, J. A. Malen, C. Majidi, *Proc. Natl. Acad. Sci. USA* **2017**, *114*, 2143–2148.
[142] S. H. Jeong, S. Chen, J. Huo, E. K. Gamstedt, J. Liu, S.-L. Zhang, Z.-B. Zhang, K. Hjort, Z. Wu, *Sci. Rep.* **2015**, *5*, 18257.
[143] M. Mohammed, A. Xenakis, M. Dickey, *Metals* **2014**, *4*, 465.
[144] S.-Y. Tang, B. Ayan, N. Nama, Y. Bian, J. P. Lata, X. Guo, T. J. Huang, *Small* **2016**, *12*, 3861.
[145] J. Thelen, M. D. Dickey, T. Ward, *Lab Chip* **2012**, *12*, 3961.
[146] B. Gol, M. E. Kurdzinski, F. J. Tovar-Lopez, P. Petersen, A. Mitchell, K. Khoshmanesh, *Appl. Phys. Lett.* **2016**, *108*, 164101.
[147] I. D. Tevis, L. B. Newcomb, M. Thuo, *Langmuir* **2014**, *30*, 14308.
[148] J. W. Boley, E. L. White, R. K. Kramer, *Adv. Mater.* **2015**, *27*, 2355.
[149] F. Hoshyargar, H. Khan, K. Kalantar-zadeh, A. P. O'Mullane, *Chem. Commun.* **2015**, *51*, 14026.
[150] L. Ren, J. Zhuang, G. Casillas, H. Feng, Y. Liu, X. Xu, Y. Liu, J. Chen, Y. Du, L. Jiang, S. X. Dou, *Adv. Funct. Mater.* **2016**, *28*, 8111.
[151] Y. Lin, C. Cooper, M. Wang, J. J. Adams, J. Genzer, M. D. Dickey, *Small* **2015**, *11*, 6397.
[152] A. Yamaguchi, Y. Mashima, T. Iyoda, *Angew. Chem.* **2015**, *127*, 13000.
[153] J. D. Eshelby, *Proc. R. Soc. A* **1957**, *241*, 376.
[154] R. W. Style, R. Boltyanskiy, B. Allen, K. E. Jensen, H. P. Foote, J. S. Wettlaufer, E. R. Dufresne, *Nat. Phys.* **2015**, *11*, 82.
[155] R. W. Style, J. S. Wettlaufer, E. R. Dufresne, *Soft Matter* **2015**, *11*, 672.
[156] F. Mancarella, R. W. Style, J. S. Wettlaufer, *Soft Matter* **2015**, *12*, 1.
[157] F. Mancarella, R. W. Style, J. S. Wettlaufer, *Proc. R. Soc. A* **2016**, *472*, 20150853.
[158] S. A. Spinelli, V. Lefèvre, O. Lopez-Pamies, *J. Mech. Phys. Solids* **2015**, *83*, 263.
[159] V. Lefèvre, O. Lopez-Pamies, *J. Mech. Phys. Solids* **2016**, *99*, 409.
[160] Vz Lefèvre, O. Lopez-Pamies, *J. Mech. Phys. Solids* **2016**, *99*, 438.
[161] C.-W. Nan, R. Birringer, D. R. Clarke, H. Gleiter, *J. Appl. Phys.* **1997**, *81*, 6692.
[162] L. Mullins, *Rubber Chem. Technol.* **1969**, *42*, 339.
[163] J. Diani, B. Fayolle, P. Gilormini, *Eur. Polym. J.* **2009**, *45*, 601.
[164] A. F. Blanchard, D. Parkinson, *Ind. Eng. Chem.* **1952**, *44*, 799.
[165] F. Bueche, *J. Appl. Polym. Sci.* **1960**, *4*, 107.
[166] R. Houwink, *Rubber Chem. Technol.* **1956**, *29*, 888.
[167] A. P. Aleksandrov, J. S. Lazurkin, *Rubber Chem. Technol.* **1946**, *19*, 42.
[168] M. Kluppel, J. Schramm, *Macromol. Theory Simul.* **2000**, *9*, 742.
[169] D. E. Hanson, M. Hawley, R. Houlton, K. Chitanvis, P. Rae, E. B. Orler, D. A. Wrobleski, *Polymer* **2005**, *46*, 10989.
[170] G. R. Hamed, S. Hatfield, *Rubber Chem. Technol.* **1989**, *62*, 143.
[171] J. P. Gong, *Science* **2014**, *344*, 161.
[172] J. P. Gong, Y. Katsuyama, T. Kurokawa, Y. Osada, *Adv. Mater.* **2003**, *15*, 1155.
[173] H. Haider, C. H. Yang, W. J. Zheng, J. H. Yang, M. X. Wang, S. Yang, M. Zrínyi, Y. Osada, Z. Suo, Q. Zhang, J. Zhou, Y. M. Chen, *Soft Matter* **2015**, *11*, 8253.

[174] M. A. Haque, T. Kurokawa, G. Kamita, J. P. Gong, *Macromolecules* **2011**, *44*, 8916.
[175] M. A. Haque, T. Kurokawa, J. P. Gong, *Polymer* **2012**, *53*, 1805.
[176] S. Lin, C. Cao, Q. Wang, M. Gonzalez, J. E. Dolbow, X. Zhao, *Soft Matter* **2014**, *10*, 7519.
[177] N. K. Singh, A. J. Lesser, *Macromolecules* **2011**, *44*, 1480.
[178] G. Lake, *Rubber Chem. Technol.* **1995**, *68*, 435.
[179] F. Carpi, D. D. Rossi, *IEEE Trans. Dielectr. Electr. Insul.* **2005**, *12*, 835.
[180] G. Gallone, F. Carpi, D. De Rossi, G. Levita, A. Marchetti, *Mater. Sci. Eng., C* **2007**, *27*, 110.
[181] T. C. Choy, *Effective Medium Theory: Principles and Applications*, Oxford University Press, Oxford, UK, **2015**.
[182] K. Lal, R. Parshad, A. S. Yadav, R. Parshad, D. C. Dube, R. Parshad, D. C. Dube, *J. Phys. D: Appl. Phys.* **1973**, *6*, 1788.
[183] Z. Hashin, S. Shtrikman, *J. Appl. Phys.* **1962**, *33*, 3125.
[184] V. Lefevre, O. Lopez-Pamies, *J. Appl. Phys.* **2014**, *116*, 134106.
[185] R. Popielarz, C. Chiang, R. Nozaki, J. Obrzut, *Macromolecules* **2001**, *34*, 5910.
[186] Z.-M. Dang, H.-Y. Wang, Y.-H. Zhang, J.-Q. Qi, *Macromol. Rapid Commun.* **2005**, *26*, 1185.
[187] L. Qi, B. I. Lee, S. Chen, W. D. Samuels, G. J. Exarhos, *Adv. Mater.* **2005**, *17*, 1777.
[188] M. Sahimi, *Phys. Rep.* **1998**, *306*, 213.
[189] M. F. Gyure, P. D. Beale, *Phys. Rev. B* **1992**, *46*, 3736.
[190] E. Garboczi, *Phys. Rev. B* **1988**, *38*, 9005.
[191] J. L. Plawsky, *Transport Phenomena Fundamentals*, CRC Press, Boca Raton, FL, USA **2014**.
[192] L. S. Lam, M. Hodes, R. Enright, *J. Heat Transfer* **2015**, *137*.
[193] Y. Hayashi, N. Saneie, G. Yip, Y. J. Kim, J. H. Kim, *Int. J. Heat Mass Transfer* **2016**, *101*, 1204.
[194] S. Mei, Y. Gao, Z. Deng, J. Liu, *J. Electron. Packag.* **2014**, *136*, 011009.
[195] P. A. Sen, C. Scala, M. H. Cohen, *Geophysics* **1981**, *46*, 781.
[196] G. K. Batchelor, R. W. O'Brien, *Proceedings of the...* **1977**, *355*, 313.
[197] A. B. Oskouyi, U. Sundararaj, P. Mertiny, *Materials* **2014**, *7*, 2501.
[198] D. J. Jeffrey, *Proc. R. Soc. A* **1973**, *335*, 355.
[199] D. R. McKenzie, R. C. McPhedran, *Nature* **1977**, *265*, 128.
[200] R. C. McPhedran, D. R. McKenzie, *Proc. R. Soc. A* **1978**, *359*, 45.
[201] T. P. Chenal, J. C. Case, J. Paik, R. K. Kramer, in *IEEE Int. Conf. Intelligent Robots and Systems (IROS)*, IEEE, Chicago IL, USA **2014**, pp. 2827–2831.
[202] C. Liu, H. Qin, P. T. Mather, *J. Mater. Chem.* **2007**, *17*, 1543.
[203] J. R. Capadona, K. Shanmuganathan, D. J. Tyler, S. J. Rowan, C. Weder, *Science* **2008**, *319*, 1370.
[204] W. Shan, S. Diller, A. Tutcuoglu, C. Majidi, *Smart Mater. Struct.* **2015**, *24*, 065001.
[205] M. A. McEvoy, N. Correll, *J. Compos. Mater.* **2015**, *49*, 1799.
[206] N. Correll, Ç. D. Önal, H. Liang, E. Schoenfeld, D. Rus, in *Experimental Robotics*, Springer, Berlin, Heidelberg, Germany, **2014**, pp. 227–240.
[207] M. Manti, V. Cacucciolo, M. Cianchetti, *IEEE Rob. Autom. Mag.* **2016**, *23*, 93.
[208] W. Shan, T. Lu, Z. Wang, C. Majidi, *Int. J. Heat Mass Transfer* **2013**, *66*, 271.
[209] J. Shintake, B. Schubert, S. Rosset, H. Shea, D. Floreano, in *IEEE Int. Conf. Intelligent Robots and Systems (IROS)*, IEEE, Chicago IL, USA **2015**, pp.1097–1102.
[210] W. Wang, H. Rodrigue, S. H. Ahn, *Composites, Part B* **2015**, *78*, 507.
[211] T. Motokawa, *Biol. Rev.* **1984**, *59*, 255.
[212] J. Trotter, J. Tipper, G. Lyons-Levy, K. Chino, A. Heuer, Z. Liu, M. Mrksich, C. Hodneland, W. S. Dillmore, T. Koob, M. M. Koob-Emunds, K. Kadler, D. Holmes, *Biochem. Soc. Trans.* **2000**, *28*, 357.
[213] W. M. Kier, *J. Exp. Biol.* **2012**, *215*, 1247.
[214] A. Hattiangadi, A. Bandyopadhyay, *Solid Freeform Fabrication Symposium* **1999**, 319.
[215] S. Dharmatilleke, H. T. Henderson, S. Bhansali, C. H. Ahn, *Proc. SPIE*, Austin, TX, USA **2000**, *4177*, 90.
[216] M. Taghavi, V. Mattoli, A. Sadeghi, B. Mazzolai, L. Beccai, *Adv. Energy Mater.* **2014**, *4*, 1.